Numerical study of thermal behaviour of building walls containing a phase change material

G. Selka*, A. N. Korti*, S. Abboudi**, R. Saim*
*Laboratory of Energetic and Applied Thermal (ETAP), Faculty of Technology, University Tlemcen, BP 230 - 13000-Tlemcen, Algeria, E-mail: g_selka@yahoo.fr
**IRTES-M3M, University of Technology of Belfort Montbeliard (UTBM), Sévenans site-90010, France,
E-mail: Said.Abboudi@utbm.fr

1. Introduction

Given the increase in the level of greenhouse gas and the climb in fossil fuel prices are the main driving forces behind efforts to improve energy efficiency. The research on the rational use of energy in buildings has shown clearly that a thorough insulation of the building envelope is required ((Alzoubi and Alshboul, 2010) [1], (Diaconu and Cruceru, 2010) [2]). The technological solutions have been introduced such as the use of latent heat (Anisure et al 2013) [3]. The principle is simple, as the temperature increases, the material changes phase (PCM) from solid to liquid. The reaction being endothermic, the PCM absorbs heat. Similarly, when the temperature decreases, the material changes phase from liquid to solid. The reaction being exothermic, the PCM release heat [4, 5]. The phase change materials used in buildings has been studied for a long time giving extensive database on the behaviour of building temperatures and energy consumptions with and without PCM ((Cabeza et al 2007) [6], (Castellón 2008)). A novel compound PCM, the shape-stabilized PCM (SSPCM), has been attracting the interests of the researchers (Inaba et Tu, 1997; Ye and Ge, 2000; Xiao et al., 2001, 2002; Zhang et al., 2006) [7-10], this PCM plate consists of paraffin as dispersed PCM and high density polyethylene (HDPE) or other materials as supporting material. the mass percentage of paraffin can be as much as 80% or so, the total stored energy is comparable with that of traditional PCMs. Zhang and Xu [11, 12] studied the thermal performance of SSPCM floor used in passive solar buildings and found that the suitable phase change temperature was roughly equal to the average indoor air temperature of sunny winter days. Kuznik et al. [13] conducted an experimental study by using a product made of 60% encapsulated PCM, in flexible panels with a thickness of 5 mm. The study was carried out over two representative days in summer: the PCM panels were superimposed on three walls in a test room, which lead to a reduction between 1°C and 2°C in the indoor air temperature. Voelker et al. [14] were interested in the effect of adding micro-encapsulated paraffin to a 30-mm gypsum plaster in a test room; the simulations, carried out over one representative week showed a potential reduction of 2C in the peak indoor air temperature. Cabeza et al [15] studied the effect of adding macro-encapsulated organic PCM in bricks walls and have evaluated through experimental measurements. In both cases, the additional thermal inertia supplied by PCM determines a reduction of 3°C in the peak indoor air temperature. Kuznik F. et al [13] have dis-

cussed the physical and thermophysical material phase change considerations on the building envelope by various measures of ownership phase change materials integrated into the building envelope. Zalewski L. et al [16] have study an experimental composite solar wall. The storage wall is made of phase change material inserted into brick-shaped package. They found the efficiency thermal of the solar wall with PCM (a 2.5 cm thick) is more efficient than a concrete wall 15 cm thick. Xing Jin et al [17] have studied the thermal performances of the double layer PCM floor, based on numerical model. The obtained results showed that the optimal melting temperatures for heating and cooling PCM are 311 K and 291 K respectively; and the optimal melting temperatures will vary with the change of the locations of the two PCM layers. Waqar A et al [18] evaluated the impact of using PCM in building from an electricity demand side perspective they observed that energy conservation gains are sensitive to the minimum and maximum temperature during 24 h period. Moreover, application of PCM in building material and potential of saving electrical energy for air conditioning during summer has also been identified as a future assessment. The purpose of our study is the thermal analysis of a passive solar building in Tlemcen (north of Algeria) with an effective heat capacity C_{eff} model. For this a real size home composed of single-story was conducted for typical day weather.

2. Physical problem

The test site on which the building is located is at 35.28°N latitude, 17.1° longitude, at an elevation of 750 m above sea level. Fig. 1 shows the building elevations plan at single-story. The substantial south-facing wall, coupled with a layer of PCM placed inside, to provide thermal storage and a horizontally concrete roof include phase change material. The windows are supposed hermetic and the external walls are composed of common red brick. The geometrical properties of the test rooms are given in Table 1.

A phase change material is coupled with brick wall in the form of sandwich. The PCM used is the paraffin. The thermal properties of different materials are presented in Table 2. In each cycle, during the charging process (sunshine hours), the PCM in the wall change its phase from solid to liquid. During the discharging process (night hours), the PCM changes its phase from liquid to solid by rejecting its heat to the ambient air in the test room. This cycle continues every day. The boundary condition on the

side south of wall and roof is considered as to combination the effects of radiation and convection
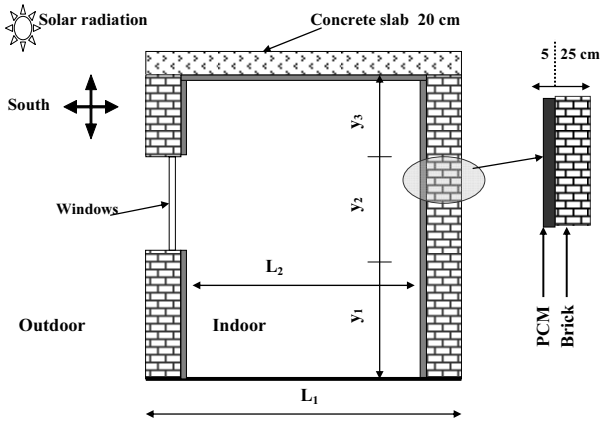

Fig. 1 Test room

The average radiation heat flux available for every one hour in *Tlemcen* City in north west of Algeria is used. For convection, the heat transfer coefficient *h* value on the outer surface is calculated based on the prevailing velocity of the wind. The boundary condition on the north wall is considered to be natural convection.

Table 1

Geometrical properties of the test rooms

y_1, m	y_2, m	y_3, m	L_1, m	L_2, m
1.0	1.0	1.0	3.6	3.0

Table 2

Thermal properties of materials

Materials	P, kg/m³	λ, W/mK	Cp, J/kgK
Paraffin	777	Eq. (8)	Eq. (7)
Concrete	2100	1.41	1000
Brick	1922	0.73	835
Glazing	2500	1.4	720

3. Mathematical formulation

The following assumptions are considered in this study:

- The thermal properties of PCM are variable in each phase (solid and liquid).
- Thermal expansion of PCM is neglected.
- Heat transfer through walls, ceiling and floor is two-dimensional.
- Thermophysical properties of building materials are constant except the PCM during melting or freezing process.
- Natural convection of the PCM during melting process and the super-cooling effect during freezing process can be ignored.

In fluid domain: Air

The governing conservation equations for unsteady, incompressible, Newtonian, two-dimensional and laminar flow are given by the following expressions:

- continuity:

$$\frac{\partial u}{\partial x} + \frac{\partial v}{\partial y} = 0 \; ; \tag{1}$$

- x-momentum:

$$\rho\left(\frac{\partial u}{\partial t} + u\frac{\partial u}{\partial x} + v\frac{\partial v}{\partial y}\right) = -\frac{\partial p}{\partial x} + \mu\left(\frac{\partial^2 u}{\partial x^2} + \frac{\partial^2 u}{\partial y^2}\right); \tag{2}$$

- y-momentum:

$$\rho\left(\frac{\partial v}{\partial t} + u\frac{\partial v}{\partial x} + v\frac{\partial v}{\partial y}\right) =$$
$$= -\frac{\partial p}{\partial y} + \mu\left(\frac{\partial^2 u}{\partial x^2} + \frac{\partial^2 u}{\partial y^2}\right) + \rho g\beta(T - T_0); \tag{3}$$

- energy:

$$\rho C_p\left(\frac{\partial T}{\partial t} + u\frac{\partial T}{\partial x} + v\frac{\partial T}{\partial y}\right) = \lambda\left(\frac{\partial^2 T}{\partial x^2} + \frac{\partial^2 T}{\partial y^2}\right). \tag{4}$$
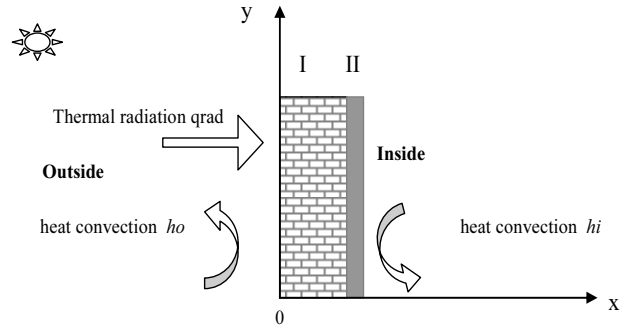

Fig. 2 Schematic of heat transfer on the exterior wall surface (I Brick, II-PCM)

The studied system is governed by the following conservative equations:

In solid domains:

brick ($i=1$), concrete ($i=2$) and glass ($i = 3$):

$$\left(\rho C_p\right)_i \frac{\partial T}{\partial t} = \lambda_i\left(\frac{\partial^2 T}{\partial x^2} + \frac{\partial^2 T}{\partial y^2}\right) \quad i=1,2,3. \tag{5}$$

In PCM domain:

The thermal behaviour of the PCM is based on the apparent capacity method:

$$\rho C_{eff} \frac{\partial T}{\partial t} = \lambda\left(\frac{\partial^2 T}{\partial x^2} + \frac{\partial^2 T}{\partial y^2}\right). \tag{6}$$

Initial conditions in fluid domain are:

$T_0 = 290$ K and $u = v = 0$.

By making the specific heat of PCM function of temperature, thermal effect of melting and solidification of PCM can be simulated. The geometry of the grid is independent of time, and the liquid/solid interface is tracked by

the definition of the specific heat in the governing equations. The specific heat is the rate of change of enthalpy with respect to temperature. The specific heat is the sum of the sensible and latent heats. In our case, the C_{eff} law, proposed by Kuznik [13], is used. It is based on the normal curve of the specific heat adapted by experimental measurements, Fig. 3 and Eq. (7):

$$C_{eff} = 10750 \ exp\left(-\frac{22.8-T}{\omega}\right) + 4252,$$
$$\begin{cases} \omega = 3 & \text{if} \quad T > 295.8 \text{ K,} \\ \omega = 4 & \text{if} \quad T \leq 295.8 \text{ K.} \end{cases} \quad (7)$$
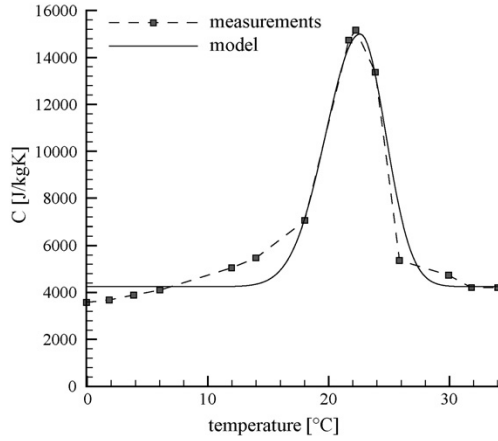

Fig. 3 Variation of apparent (effective) heat capacity with temperature [13]

The curve corresponding to Eq. (7) is plotted in Fig. 3. As one can observe, the melting process starts at $T = 16°C$ (289 K) and ends at $27°C$ (300 K); the peak temperature is $T = 22.8°C$ (295.8 K), after which melting is completed quite rapidly.

The thermal conductivity λ is defined by the following relations:

$$\lambda = \begin{cases} \lambda_S & \text{if} \quad T \leq 22.8°C; \\ \lambda_l & \text{if} \quad T > 22.8°C. \end{cases} \quad (8)$$

Boundary conditions:

All walls of the studied rooms are submitted to convective heat transfer with ambient, except the bottom wall. The radiation heat flux is added at the south wall and the concrete roof:

$$Q = h(T - T_a) + \varphi(t), \quad (9)$$

where $\varphi(t)$ is the solar radiation heat flux according to the typical day of Tlemcen (Fig. 4, b) is the convection heat transfer coefficient due to wind, recommended by McAdams [19]:

$$h = 5.67 + 3.86 v_w, \quad (10)$$

where v_w is the velocity wind (Fig. 4, c).

The Algerian typical day weather 12 of May in Tlemcen (Altitude 750 m, Latitude 35°28'N and Longitude 17°1') is chosen as the outdoor climate data. The hourly variation of outdoor air temperature and solar radiation on the south wall is shown in Fig. 4. The average outdoor air temperature is 296 K.
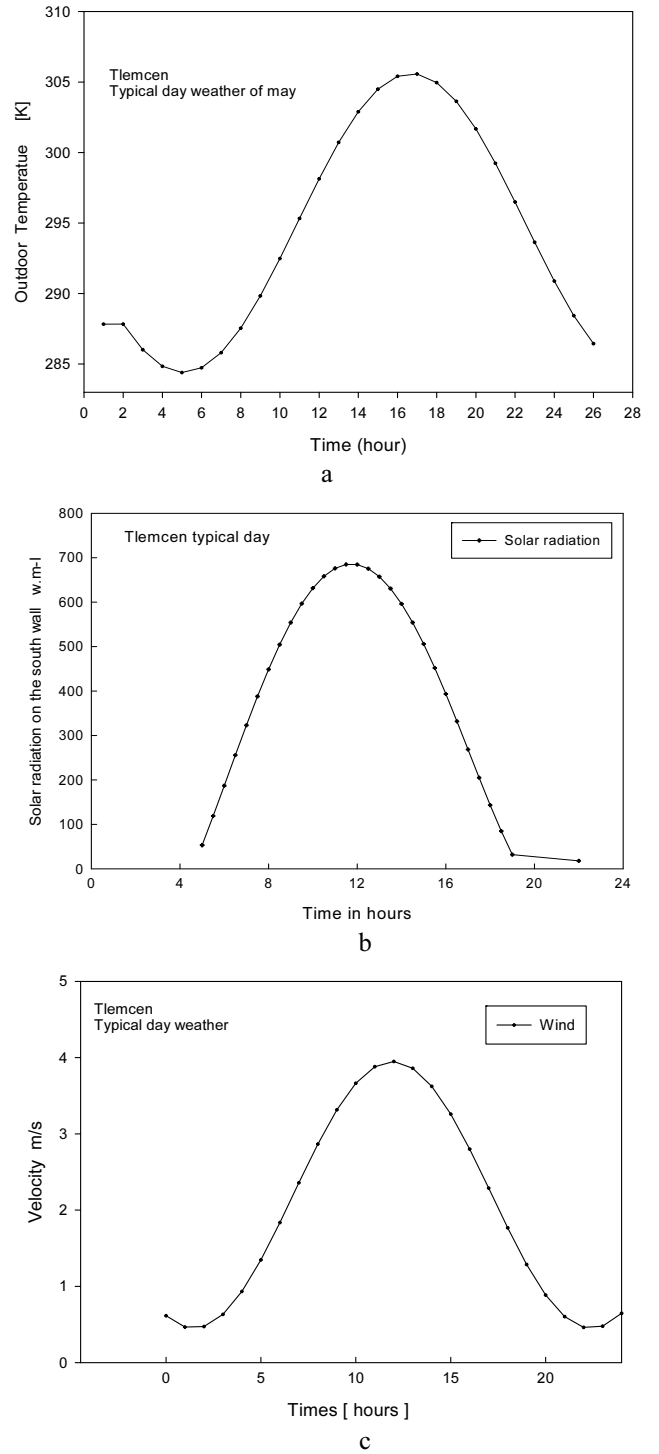

a

b

c

Fig. 4 Hourly variation of outdoor: a - air temperature, b - solar radiation, c - velocity wind

4. Results and discussion

The commercial CFD software package, *FLUENT*, which is based on the finite volume approach was used for solving the set of governing equations. A user define function (UDF) is used to introduce the unsteady profiles of boundary conditions. Fluent provides the flexibility in choosing discretization schemes for each governing equation. The discretised equations, along with the initial and boundary conditions, were solved using the segregated solution method to obtain a numerical solution. Using the segregated solver, the conservation of mass and momentum were solved iteratively and the SIMPLE algo-

rithm was used to ensure the momentum and mass conservation equations [20]. The convergence criterion was set equal to 10^{-7} for all parameters.

Before the numerical analysis, the grid-independency of the test rooms system was simply checked using a different number of grids. The system was finally divided in to 9900 cells with 10404 nodes in consideration of grid-independency and calculating efficiencies.

5. Experimental investigation

The physical system considered is a composite wall filled with PCM placed between the roof top slab and the bottom concrete slab, which form the roof of the PCM room. During sunshine hours, the PCM changes its phase from solid to liquid. During the night hours, the PCM passes from the liquid to solid phases (solidification) by

$$k_1 \left.\frac{\partial T_1}{\partial x}\right|_{x=0} = q_{rad} + h_0 \left(T_\infty - T_{x=0}\right)$$

$$k_3 \left.\frac{\partial T_3}{\partial x}\right|_{x=L} = h_i \left(T_{x=L} - T_{room}\right)$$
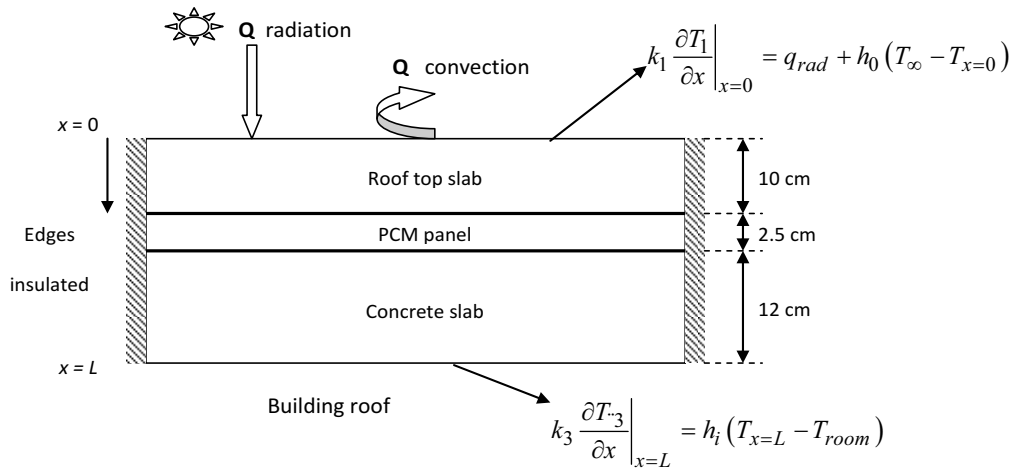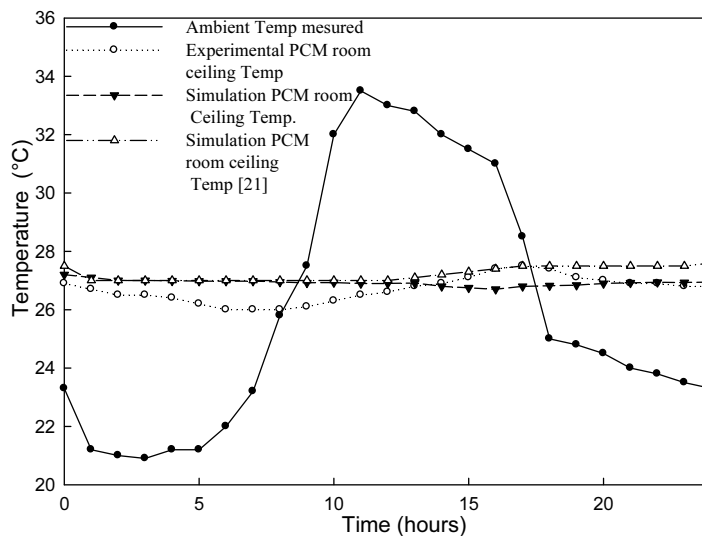
Fig. 5 Presentation of the building roof

Fig. 6 Experimental and simulated temperature of the ceiling in the PCM and non-PCM room

rejecting its heat to the ambient and to the air inside the room. Initially, the composite wall is maintained at a uniform temperature 300 K. The boundary conditions and the properties of the PCM are given in the ref. [21].

The Fig. 6 shows the experimental and simulated evolutions of the ceiling temperature of the PCM room during 24 h of daytime. There is good agreement between the measurements and the numerical approach uses effective heat capacity C_{eff} model. The maximum temperature difference between the experimental and the numerical obtained curves is about 0.60°C. This shows that the thermal response of the room is correctly reproduced by the thermal model.

The Fig. 7 shows the evolution of the temperature fields inside the test room at 06:00, 12:00, 18:00 and

24:00. The outside temperature varies from 288 to 306 K. We can see that the peak temperature within the test room moves in versus time. During the solar radiation such as at 12:00 there is a warming of the test room and more intense near the windows due to the conductivity of glazing. It also reports a horizontal thermal gradient is observed near the south-facing wall and advance inwards.

The evolution of the temperature is higher in the south than the north wall because the solar radiations are more important on the south wall.

At 18:00, the temperature inside the test room continues to increase despite the temperature outdoor and solar radiation decreases. This phenomenon is due to the heat sensible stored in the wall of test room and the heat latent stored in the PCM.
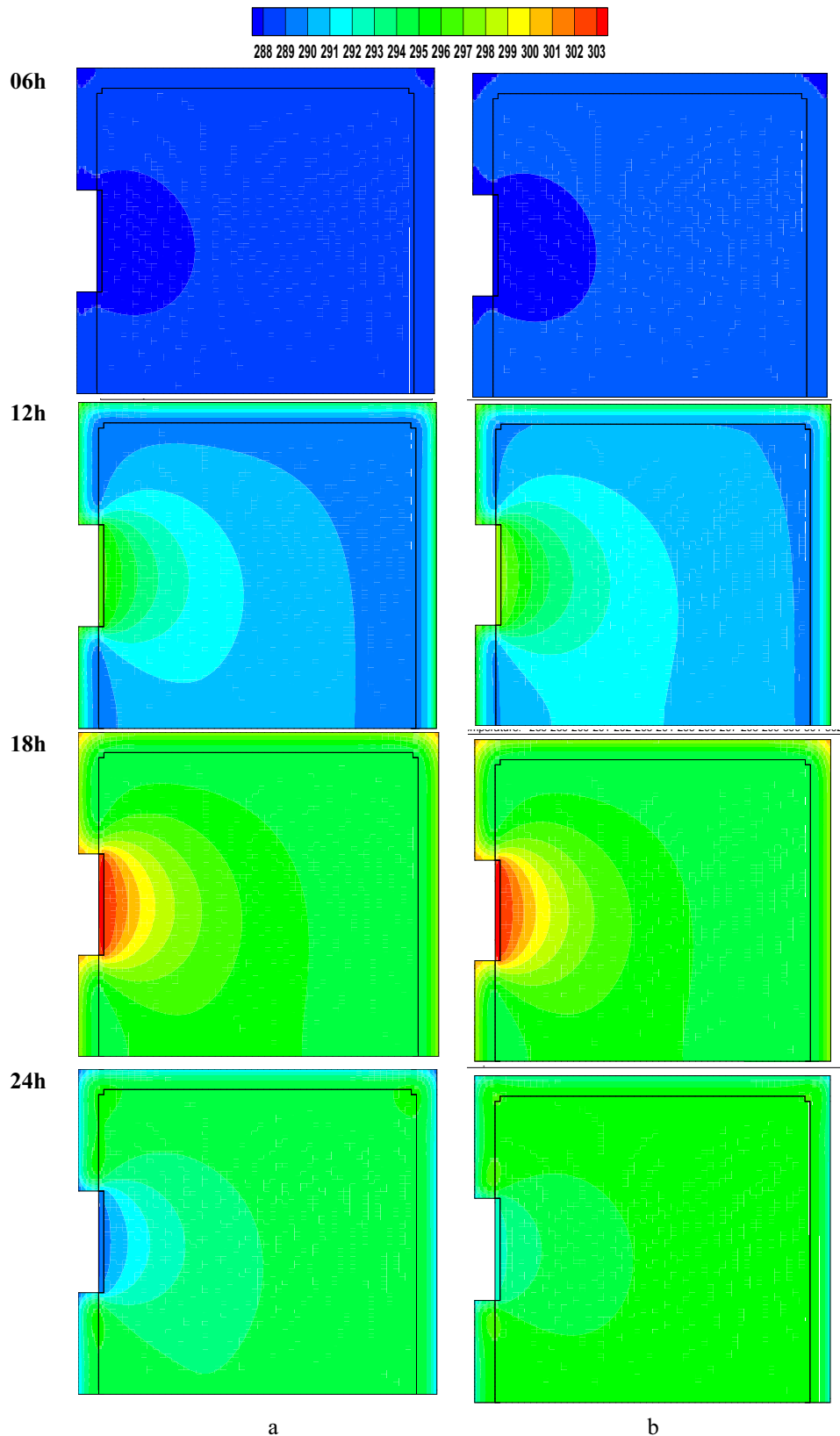
Fig. 7 Temperature contour: a - with PCM; b - without PCM

At 24:00, the temperature at the interior of the room is more homogeneous (approximately 297.2 K). It also records the start of cooling at the roof due the heat energy exhaustion in the PCM.

Therefore, there is a significant influence of the thermal conductivity of glazing thus the material of roof should be chosen properly to provide comfort air temperature in the room.

Fig. 8 shows the evolution of the air temperature during six days. The interior temperature is stabilized between 292 K and 295.8 K at 24:00 of days. The temperature differences between test room with and without PCM exceed 1.2°C. It can be seen that the maximal temperature reached is 296.2 K (296.8 K in the test room without PCM) after 24 h and 296.15 K (297.2 K in the case without PCM) after 48 h, respectively. The PCM can reduce considerably
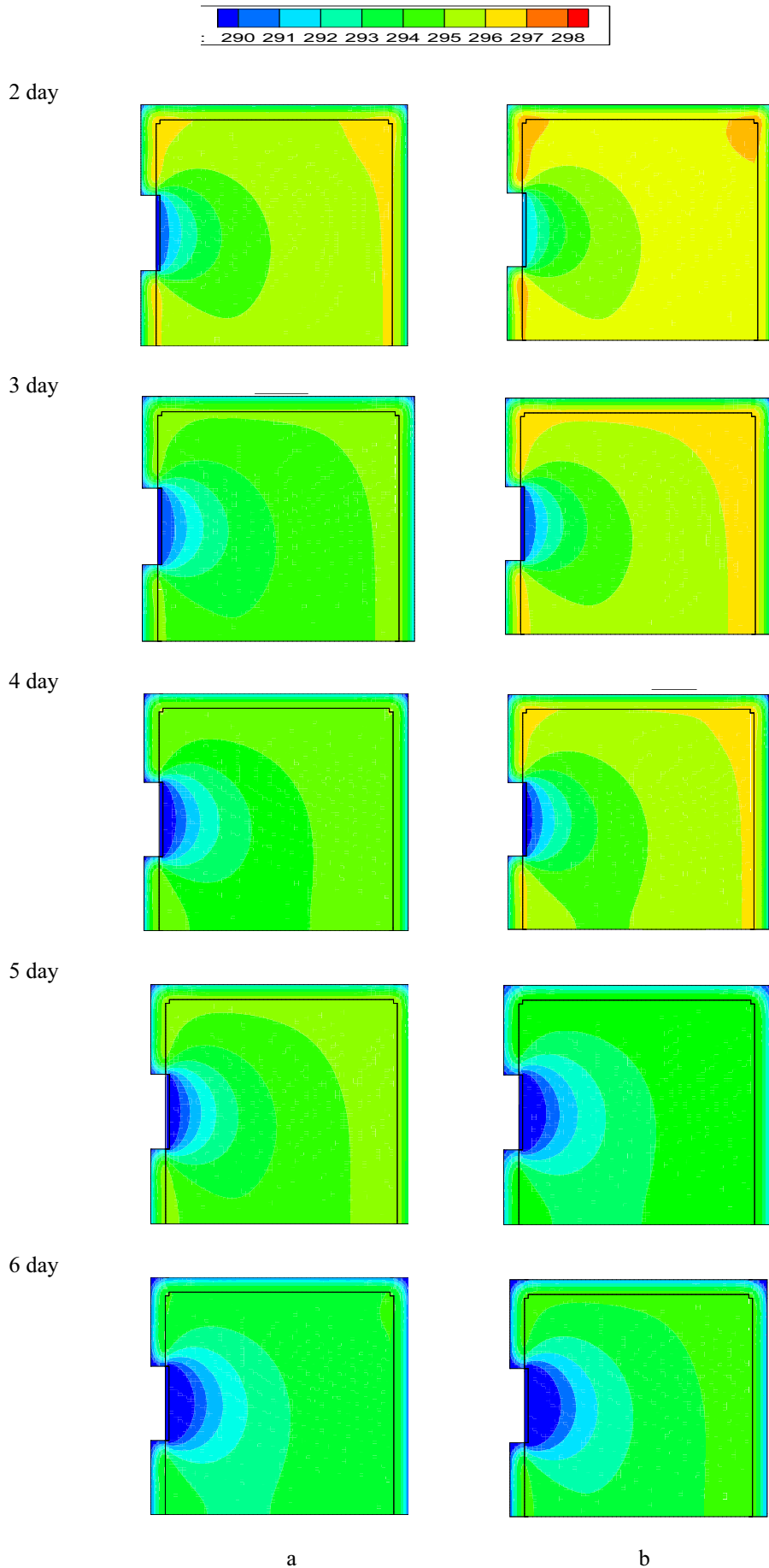
Fig. 8 Evolution of the air temperature during six days: a - with PCM; b - without PCM

the interior temperature. The PCM composite walls allow enhancing the thermal comfort of the test room under these conditions. The maximum air temperature is decreased by about 6 to 8 K and the minimum increased by about 3 to 6 K. Another notable effect is the natural convection enhancement allowing to have a better mixing concerning the air in the test room and decreasing the temperature gradient.

To compare the performances storing energy savings, a numerical simulation with the PCM is compared to a simulation without PCM as shown Fig. 9.
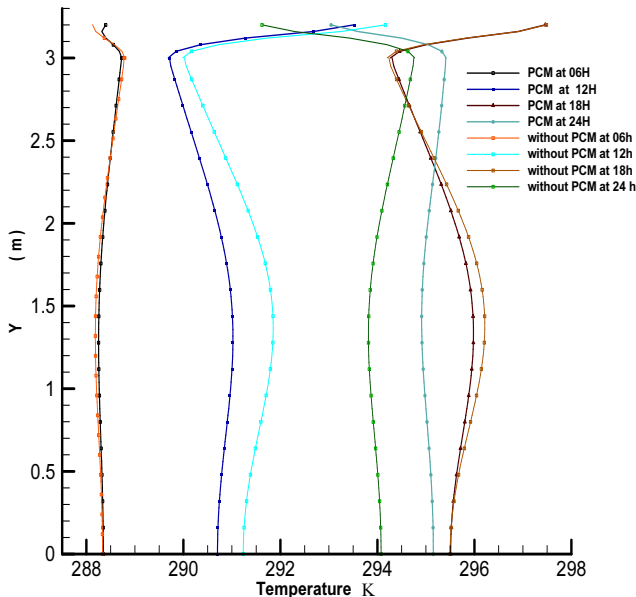

Fig. 9 Temperatures profiles at different times (6, 12, 18 and 24 h o'clock)

Fig. 9 illustrates the temperature profiles at different times (06, 12, 18 and 24 h o'clock) in the air ambiance ($x = 1.60$ m). At 06 h o'clock, we note the beginning of cooling in the test room, the ambient temperature inside the test room is almost the same with and without PCM.

At 12 o'clock, the temperature of the test room (with PCM) reached 291 K due to the intense solar radiation. However, the air temperature in the room without PCM is higher than 291.8 K. At this time, the PCM is completely solid.

At time 18 h o'clock, we see the increase of temperature in the test rooms at approximately 296 K (with PCM), and 296.35 K (without PCM). The PCM temperature is in the phase change region and become partially liquid. The PCM begins to absorb the latent heat

The air temperature in the test rooms begins to decrease and indicates that the heat gain is effectively absorbing through melting /solidification process.

At time 24 h o'clock, the convection heat exchange is strongly reduced between the outdoor and the inside ambient. The air temperature in the test rooms begins to decrease and indicates that the heat gain is effectively absorbing through melting / solidification process. However, the air temperature in the test room with PCM is 295 K but the air temperature in the test room without PCM is lower than 294 K. This proves that the PCM acts as a thermal energy accumulator and regulates more perfectly the ambiance temperature.

Fig. 10 shows temperature evolutions at test room, and outdoor during 06 days (144 h) with PCM and without PCM. We can see that the amplitude of the temperature variation of test room without PCM is higher than that of the temperature variation of test room with PCM. However, a time shift can be observed around 6.3 h (with PCM) and 2 h (without PCM) between the outdoor and the inside temperatures in the test room. The time shift with PCM is higher than without PCM. This indicates clearly the energy storage process associated with phase changes. The maximum of the temperature is about 306 K for outdoor, 297.95 K (with PCM) and 300.1 K (without PCM) for test room And the minimum of the temperature is about 284.5 K for outdoor, 292.6 K (with PCM) and 289.9 K (without PCM) for test room. This proves clearly that the incorporation of PCM in walls allows us to smooth out fluctuations in the internal ambient temperature, reduce daily energy consumption and enhances the thermal comfort during the daytime.
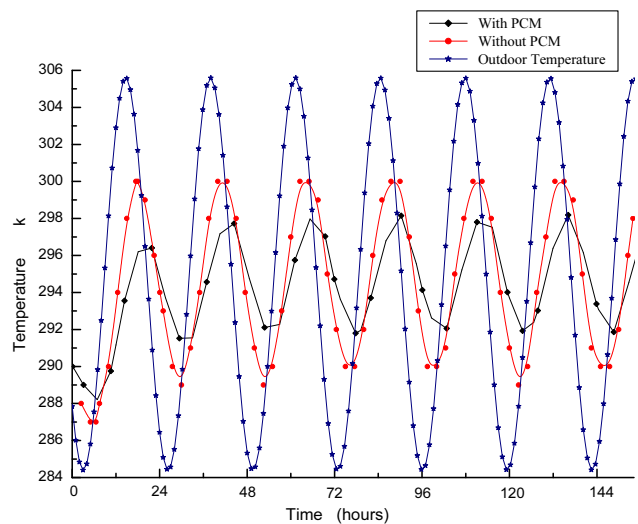

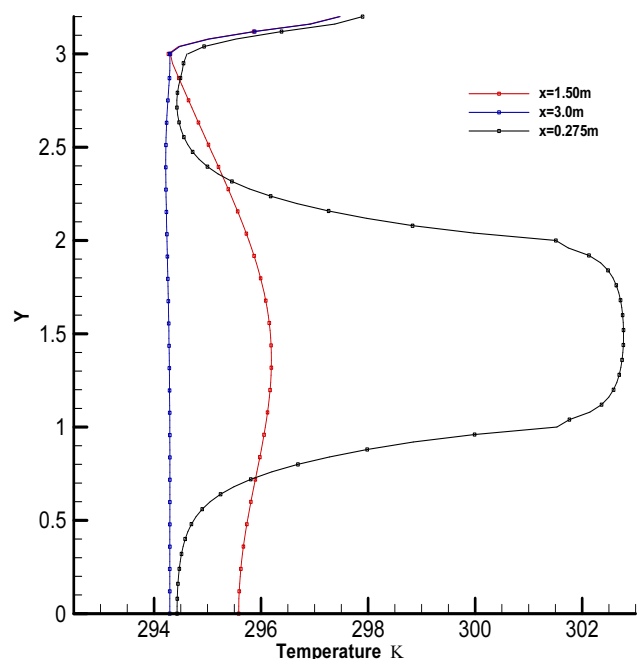Fig. 10 Temperature evolutions at test rooms, and outdoor

Fig. 11 Evolutions of temperatures at different positions ($x = 0.275$ m, $x = 1.5$ m and $x = 3.0$ m)

Fig. 11 presents the evolutions of temperatures at different positions in the south ($x = 0.275$ m), north ($x = 3.0$ m) PCM walls and in the ambiance ($x = 1.5$ m). The temperature profile of the south PCM wall presents two peaks due to the presence of the thermal bridging (glazing). We note also that the south wall temperature is higher than the ambiance and the north wall temperatures due to the solar radiation incident.

It is interesting to note that the evolution of the ambient temperature profile in the north wall is more stable than the south wall temperature due to the not presence of the window. We can notice that the maximum temperature peaks are near the windows, clearly indicating the presence of thermal bridge.

6. Conclusion

The purpose of this work is to present a thermal performance of phase change material (PCM) integrate in a passive solar building in Tlemcen. The numerical approach based on the effective heat capacity C_{eff} with realistic outdoor climatic conditions of Tlemcen city.

It was shown that the utilization of PCM layer in a passive solar building may reduce the maximum test room temperature by about 6 to 8 K during the daytime and increase the minimum temperature by about 8 K during the night which reduces the heating load significantly.

Secondly, the results show that, in the present conditions, typical in Tlemcen, the optimal comfort temperature is about 296.8 K corresponds to the human comfort in buildings. The influence of the melting temperature of the PCM is significant at ambient temperature should be chosen properly to avoid the occurrence of the overheating.

It is interesting to note that the excess heat is stored in the PCM and a temperature gradient is created near in the windows of test room. This improved thermal comfort is more important if we reinforce the isolation of the window in the test. Finally the use of PCM in building envelope for thermal storage could lead to lower consumption of energy resource, which provides benefits to both economic and environmental aspects.

References

1. **Alzoubi, H.**; **Alshboul, A.** 2010. Low energy architecture and solar rights: restructuring urban regulations, view from Jordan, Renewable Energy 35(2): 333-342. http://dx.doi.org/10.1016/j.renene.2009.06.017.

2. **Diaconu, B.**; **Cruceru, M.** 2010. Novel concept of composite phase change material wall system for year round thermal energy savings, Energy and Buildings, 42 (10):101-107. http://dx.doi.org/10.1016/j.enbuild.2010.05.012.

3. **Anisur, M.R.**; **Mahfuz, M.H.; Kibria, M.A.; Saidur, R.; Metselaar, I.H.S.C.; Mahlia, T.M.I**. 2013. Curbing global warming with phase change materials for energy storage, Renewable and Sustainable Energy Reviews18: 23-30. http://dx.doi.org/10.1016/j.rser.2012.10.014.

4. **Kuznik, F.**; **David, D.; Johannes, K.; Roux, J.J**. 2011. A review on phase change materials integrated in building walls. Renewable and Sustainable Energy Reviews 15(1): 379-391. http://dx.doi.org/10.1016/j.rser.2010.08.019.

5. **Farid, M.M.**; **Khudhair, A.M.; Razack, S.A.K.; Al-Hallaj,** S. 2004. A review on phase change energy storage: materials and applications. Energy Convers Manage 45:1597-1615. http://dx.doi.org/10.1016/j.enconman.2003.09.015.

6. **Cabeza, L.F.**; **Castellón, C.**; **Nogués, M.; Medrano, M.; Leppers, R.**; **Zubillaga, O**. 2007, Use of micro-encapsulated PCM in concrete walls for energy savings. Energy and Buildings 39(2): 113-119. http://dx.doi.org/10.1016/j.enbuild.2006.03.030.

7. **Inaba, H.; Tu, P**. 1997. Evaluation of thermophysical characteristics on shape-stabilized paraffin as a solid–liquid phase change material. Heat Mass Transfer 32: 307-312. Available from Internet: http://link.springer.com/article/10.1007%2Fs002310050126.

8. **Xiao, M.**; **Feng, B.; Gong, K.C**. 2001. Thermal performance of a high conductive shape-stabilized SSPCM thermal storage material. Solar Energy Materials and Solar Cells 69: 293-296. http://dx.doi.org/10.1016/S0927-0248(01)00056-3.

9. **Zhang, Y.P.**; **Lin, K.P.; Yang, R.; Di, H.F.; Jiang, Y**. 2006. Preparation, thermal performance and application of shape-stabilized PCM in energy efficient buildings. Energy and Buildings 38, 1262-1269. http://dx.doi.org/10.1016/j.enbuild.2006.02.009.

10. **Ye, H.**; **Ge, X.S**. 2000, Preparation of polyethylene-paraffin compound as a form-stable solid-liquid phase change material. Solar Energy Materials and Solar Cells 64, 37-44. http://dx.doi.org/10.1016/S0927-0248(00)00041-6

11. **Xu X.; Zhang YP.**; **Lin KP.; Di HF, Yang R**. 2005 Modeling and simulation on the thermal performance of shape-stabilized phase change material floor used in passive solar buildings. Energy and Buildings 37(10): 1084-1091. http://dx.doi.org/10.1016/j.enbuild.2004.12.016.

12. **Zhang, Y.P.**; **Xu, X.; Di, H.F.; Lin, K.P.; Yang, R**. 2006. Experimental study on the thermal performance of the shape-stabilized phase change material floor used in passive solar buildings. Journal of Solar Energy Engineering ASME 128(2): 255-257. http://dx.doi.org/10.1115/1.2189866.

13. **Kuznik, F.**; **Virgone, J.; Roux, J.J**. 2008. Energetic efficiency of room wall containing PCM wallboard: a full-scale experimental investigation. Energy and Buildings 40(2): 148-156. http://dx.doi.org/10.1016/j.enbuild.2007.01.022.

14. **Voelker, C.**; **Kornadt, O.; Ostry, M**. 2008. Temperature reduction due to the application of phase change materials. Energy and Buildings 40(5):937-944. http://dx.doi.org/10.1016/j.enbuild.2007.07.008.

15. **Khudhair, A.**; **Farid, M.** A review on energy conservation in building applications with thermal storage by latent heat using phase change materials, Energy Conversion and Management 2004, 45(2), 263-275. http://dx.doi.org/10.1016/S0196-8904(03)00131-6.

16. **Zalewski, L.; Joulin, A.; Lassue, S.; Chartier, T**. 2010. Caractérisation thermophysique du comportement de matériaux à changement de phase à échelle macro. Congrès Français de Thermique, SFT 2010, Touquet, 25-28 mai.

http://www.sft.asso.fr/Local/sft/dir/user-3775/documents/actes/Congres_2010/communications/163.pdf.

17. **Xing, J.; Xiaosong, Z**. 2011. Thermal analysis of a double layer phase change material floor, Applied Thermal Engineering 31: 1576-1581.
http://dx.doi.org/10.1016/j.applthermaleng.2011.01.023

18. **Waqar, A.Q.; Nirmal-Kumar, C.N.; Mohammad, M.F**. 2011. Impact of energy storage in buildings on electricity demand side management, Energy Conversion and Management 52: 2110-2120.
http://dx.doi.org/10.1016/j.enconman.2010.12.008

19. **Mc Adams, W.H**. 1954. Heat Transmission, third edition, McGraw-Hill, New York.

20. **Patankar, S.V.** 1980. Numerical Heat Transfer and Fluid Flow, Hemisphere/McGraw-Hill, New York.

21. **Pasupathy, A. et al**. 2008, Experimental investigation and numerical simulation analysis on the thermal performance of a building roof incorporating phase change material (PCM) for thermal management Applied Thermal Engineering 28: 556-565.
http://dx.doi.org/10.1016/j.applthermaleng.2007.04.016

G. Selka, A.N. Korti, S. Abboudi, R. Saim

PASTATŲ SIENŲ TURINČIŲ MEDŽIAGŲ SU KINTANČIA FAZINE BŪSENA ŠILUMINIŲ SAVYBIŲ SKAITMENINĖ ANALIZĖ

R e z i u m ė

Šiame darbe pateikiama medžiagų su kintančia fazine būsena šiluminių savybių 2D skaitmeninė analizė siekiant gerinti šilumines pastatų Tlemcene (šiaurės Alžyras) charakteristikas eilinę žinomos temperatūros, saulės radiacijos ir vėjo greičio dieną. Speciali parafino medžiaga buvo įvesta į plytų sieną norint sumažinti kambario temperatūrą dienos metu. Skaitmeninis priartėjimas naudoja šilumos talpio C_{eff} modelį su realiomis klimato sąlygomis Tlemceno, Alžyras, mieste. Skaitmeniniai rezultatai rodo ženklų, nuo 6°C iki 8°C temperatūros sumažėjimą saulės apšviestame bandymų kambario viduje. Dėl to sumažėja energijos poreikis kondicionavimui, o tai suteikia tiek ekonominę tiek aplinkosauginę naudą.

G. Selka, A.N. Korti, S. Abboudi, R. Saim

NUMERICAL STUDY OF THERMAL BEHAVIOUR OF BUILDING WALLS CONTAINING A PHASE CHANGE MATERIAL

S u m m a r y

In the present work we presents 2D numerical study of using a phase change material to improve thermal performance of building in Tlemcen (north of Algeria) for typical day chosen with known outdoor temperature, solar radiation and wind velocity. A specific paraffin material was placed in brick wall to reduce the room temperature during a daytime. The numerical approach uses effective heat capacity C_{eff} model with realistic outdoor climatic conditions of Tlemcen city, Algeria. The numerical results show a significant temperature reduction inside the studied solar test room, about 6°C to 8°C and therefore, the energy consumption due to air conditioning is reduced which provides benefits to economic and environmental aspects.